



Fate of nutrients during hydrothermal treatment of food waste

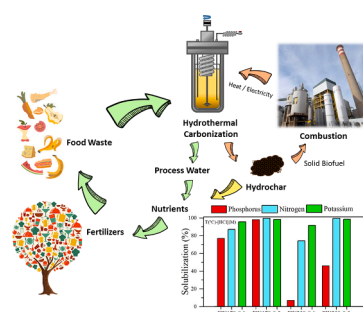
Andres Sarrion^{*}, Elena Diaz, M. Angeles de la Rubia, Angel F. Mohedano

Department of Chemical Engineering, Faculty of Science, Universidad Autónoma de Madrid, Campus de Cantoblanco, 28049 Madrid, Spain

HIGHLIGHTS

- Optimization of nutrient recovery from food waste by hydrothermal carbonization (HTC)
- Acid-mediated HTC improved hydrochar properties as a solid fuel.
- Low temperature (170 °C) and acid-mediated (0.5 M HCl) HTC favoured nutrient extraction to process water.
- Acid-mediated HTC increased the respective extraction of N and P as $\text{NH}_4\text{-N}$ and $\text{PO}_4\text{-P}$.

GRAPHICAL ABSTRACT



ARTICLE INFO

Keywords:

Biomass valorization
Hydrochar
Hydrothermal carbonization
Nutrient recovery
Food waste

ABSTRACT

Hydrothermal carbonization was evaluated as a food waste valorization strategy to obtain hydrochar and recover nutrients. In the hydrothermal treatment, the temperature (170–230 °C), reaction time (5–60 min), and addition of HCl (0.1–0.5 M) during the reaction were analyzed. Compared to the feedstock, hydrochar showed an increase in fixed carbon (greater than 45%) and a decrease in ash content (<7%), along with a higher heating value (18.6–26.2 MJ/kg), which would allow for its application as a biofuel for industry according to ISO/TS 17225–8. The hydrochar obtained using plain carbonization showed 75% P and 40% N of the feedstock content, whereas the HCl-mediated treatment (0.5 M) solubilized most of the P, K, and N in the process water (98% P as $\text{PO}_4\text{-P}$, 98% K, and the total N content as $\text{NH}_4\text{-N}$ (16%) and organic-N) operating at 170 °C for 60 min.

1. Introduction

Currently, one of the main social problems is the inadequate management of waste, which has several negative impacts on the environment, such as soil and water pollution, excessive depletion of natural resources, degradation of ecosystems, and progressive worsening of health (Vallero, 2019). In 2019, more than 2×10^9 tonnes of municipal solid waste were generated worldwide, and it is estimated that this amount will increase up to 70% by 2050, with 44% corresponding to the

organic fraction of municipal waste (OFMW), which is mainly composed of food waste (World bank, 2018). This high increase is attributed to rapid population growth, high urban overcrowding, and/or inefficient production systems that shorten the lifetime of the materials (Tang et al., 2020). The current European legislation related to biowaste management establishes some actions to minimize the impact of such waste on the environment through a circular economic policy based on reduction of the carbon footprint of waste through useful knowledge of eco-friendly management (European Commission, 2020).

^{*} Corresponding author.

E-mail address: andres.sarrion@uam.es (A. Sarrion).

<https://doi.org/10.1016/j.biortech.2021.125954>

Received 27 July 2021; Received in revised form 8 September 2021; Accepted 12 September 2021

Available online 20 September 2021

0960-8524/© 2021 The Author(s).

Published by Elsevier Ltd.

This is an open access article under the CC BY-NC-ND license

(<http://creativecommons.org/licenses/by-nc-nd/4.0/>).

Food waste consists mainly of organic compounds and mineral salts (Panigrahi and Dubey, 2019), including a significant concentration of essential nutrients (mainly phosphorus, nitrogen, and potassium). The scarcity of these nutrients from natural sources makes it necessary to find new ways of recovery (Zhao et al., 2018). These nutrients are the main components of agricultural fertilizer (Ostadi et al., 2020), which is crucial to ensuring sufficient production to meet the needs of a growing population in the coming years (up to 9.7×10^6 people in 2050) (Kjerstadius et al., 2015). Furthermore, the opportunity to recover nutrients from food waste is coupled with achieving the current European Directive 2018/851 (European Commission, 2018), which is focused on recovering more than 50% of biowaste-based materials through recycling by 2025 and managing them through a non-conventional alternative to landfilling.

In addition to biological processes (mainly composting and anaerobic digestion), thermochemical conversion is a feasible route for handling food waste. In this framework, hydrothermal carbonization (HTC) is an emerging technology that allows for the recovery of nutrients from biowaste that has a high degree of moisture, together with subsequent energy valorization of the feedstock. HTC is a thermochemical process in which the wet feedstock is treated at 170–250 °C and with low residence times (5–240 min) under self-generated pressure. Through hydrolysis, condensation, aromatization, dehydration, and decarboxylation reactions, a carbon-rich solid product known as hydrochar, with fuel properties similar to those of lignite, process water containing inorganic salts and organic compounds, and a gaseous stream consisting mainly of CO₂ are obtained (Kumar et al., 2018). Although these reactions can be endothermic or exothermic, the HTC process is slightly exothermic in this temperature range, as it is mainly governed by dehydration and decarboxylation reactions, which decrease both the oxygen and hydrogen content of the feedstock (Berge et al., 2011; Funke and Ziegler, 2011). Owing to the physical and energetic properties of hydrochar, its main potential applications include its use as solid fuel (He et al., 2013; Sharma et al., 2019), catalyst support (Ge et al., 2020; Tang et al., 2020), activated carbon precursor (Diaz et al., 2019; Fernandez et al., 2015), soil amendment material (Xia et al., 2020), and energy storage in batteries, fuel cells, or supercapacitors (Niu et al., 2020; Wilk et al., 2019), as well as direct use as an alternative nutrient source (Becker et al., 2019).

Different strategies to solubilize nutrients by hydrothermal treatments from several types of biomass waste have been described in previous works. The simplest strategy is based on the direct acid washing of biomass (Shiba and Ntuli, 2017; Szögi et al., 2015). Some authors have examined biomass nutrient recovery using HTC by promoting nutrient leaching into the process water (Ekpo et al., 2015; Idowu et al., 2017) or their concentration in the hydrochar (Becker et al., 2019; Heilmann et al., 2014). Acid-mediated HTC as an option to facilitate the release of N and P from biomass has been scarcely studied, despite the interesting results obtained by Dai et al. (2017), Ekpo et al. (2015), and Qaramaleki et al. (2020). The aim of this work was therefore to study the fate of nutrients (N, P, and K) between the hydrochar and the process water obtained in the HTC of food waste at several temperatures (170–230 °C), residence times (5–60 min), and with the addition of HCl (0.1–0.5 M) during the process.

The recovery of concentrated nutrients in the process water can be carried out by different physicochemical processes. In the case of P the most commonly used method is chemical precipitation in the form of struvite, when magnesium salts are used as a reagent, or as calcium phosphates or hydroxyapatite, using calcium salts as a reagent (Cieřlik and Konieczka, 2017). This method allows obtaining high recovery yields and generates high quality P minerals that can be directly applied in agriculture, improving soil characteristics (Cieřlik and Konieczka, 2017). In the case of nitrogen, air ammonia stripping is suitable for process waters with very high ammonia concentration (3–4 g/L). At low concentrations, ammonium can precipitate together with phosphate in the form of struvite (Yu et al., 2017). Although K is highly soluble and

not usually extracted from the aqueous phase, it is essential for plant growth and, therefore, several works focus on the use of HTC process water as irrigation water because it contains large amounts of nutrients and a mixture of organic and inorganic compounds that can stimulate plant growth (Celletti et al., 2021).

2. Materials and methods

2.1. Food waste

Food waste was collected from a local management plant operating on a food distribution platform (Madrid, Spain). The feedstock was composed mainly of fruit and vegetable waste, with a small amount of meat waste. The raw food waste was ground and stored in 1.5 kg portions at –20 °C to ensure its preservation. In each experiment, the moisture content of defrosted portions of the food waste was measured (91–93 wt%). Table 1 lists the values of the main feedstock characteristics.

2.2. Hydrothermal carbonization experiments

Hydrothermal experiments were carried out in an electrically heated ZipperClave® stirred pressure vessel (4 L). In each run, the reactor was loaded with 1.5 kg of defrosted feedstock. The operating temperature (170–230 °C) was reached by heating the reactor at a rate of 3 °C/min and holding at the selected temperature for 1 h. The effects of temperature and HCl addition (0.1–0.5 M) were studied using response surface methodology based on a fractional factorial design with a duplicate central point. Using Minitab 19 software, three acid-free experiments and six acid-mediated experiments (four factorial points and two replicates of the central point) were performed. The hydrochar was denoted by the carbonization temperature (i.e., HC170) and the addition of HCl (i.e., HC170-0.1). Each experiment was performed in duplicate.

Samples of the process water (40 mL) were withdrawn from the reactor at 5, 15, 30, and 60 min using a sample collection system. The reaction was stopped after 60 min by cooling with an internal heat exchanger using tap water. The slurry (hydrochar plus process water) was then separated by filtration using 250 µm membrane vacuum filters. Hydrochar was obtained by oven drying the solid fraction overnight at 105 °C with subsequent grinding and sieving to a particle size between 100 and 200 µm. The process water was filtered through 0.45 µm Scharlab glass filters and stored at 4 °C. The process water was denoted by the carbonization temperature (i.e., PW170) and the addition of HCl (i.e., PW170-0.1). The mass yield of hydrochar (Y_{HC}) was defined as the weight ratio of recovered hydrochar (W_{HC}) to raw food waste (W_{FW}) on a dry basis (Equation (1)).

$$Y_{HC}(\%) = (W_{HC}/W_{FW}) \cdot 100 \quad (1)$$

The yield of process water (Y_{PW}) was calculated as the ratio of the volume of process water recovered (V_{PW}) to the liquid volume of the raw food waste (V_{FW}) (Equation (2)).

$$Y_{PW}(\%) = (V_{PW}/V_{FW}) \cdot 100 \quad (2)$$

2.3. Phosphorus, nitrogen, and potassium leaching from the hydrochar

A sample of hydrochar (10 g) from acid-free HTC (170–230 °C) was treated with 100 mL of 0.5 M HCl using an orbital shaker for 2 h to extract P, N, and K. The resulting leachate and washed hydrochar (WHC) were separated by vacuum filtration (pore size 0.45 µm) for further analysis.

2.4. Analytical methods

The elemental compositions (C, H, N, and S) of the process water, leachate, and hydrochar samples (including washed hydrochar) were

Table 1

Main characteristics of feedstock and hydrochar from HTC (dry basis).

Sample	Proximate analysis (wt.%)				Ultimate analysis (wt.%)					P (wt.%)	K (wt.%)	HHV (MJ/kg)
	Yield	FC	VM	Ash	C	N	S	H	O ^a			
Feedstock	–	20.6 ± 0.2	67.6 ± 0.1	11.8 ± 0.1	44.5 ± 0.3	3.1 ± 0.2	0.2 ± 0.0	6.1 ± 0.8	34.3 ± 0.2	0.5 ± 0.0	3.8 ± 0.2	18.9 ± 0.1
HC170	80.4 ± 0.5	27.3 ± 0.3	60.1 ± 0.2	12.6 ± 0.2	46.2 ± 0.3	1.7 ± 0.1	0.2 ± 0.0	5.9 ± 0.2	33.4 ± 0.2	0.4 ± 0.1	0.7 ± 0.1	19.4 ± 0.2
HC200	67.7 ± 2.2	28.6 ± 0.4	57.8 ± 1.6	13.6 ± 0.3	48.6 ± 0.1	2.0 ± 0.2	0.2 ± 0.0	5.7 ± 0.2	29.9 ± 0.2	0.7 ± 0.0	1.4 ± 0.2	20.3 ± 0.2
HC230	61.2 ± 1.6	29.5 ± 0.9	56.2 ± 0.2	14.3 ± 0.2	54.8 ± 0.9	2.3 ± 0.3	0.2 ± 0.0	6.1 ± 0.1	22.3 ± 0.1	0.8 ± 0.2	1.6 ± 0.2	23.7 ± 0.1
HC170-0.1	55.5 ± 1.2	29.5 ± 0.5	62.7 ± 0.2	7.8 ± 0.2	45.8 ± 0.1	1.2 ± 0.0	0.2 ± 0.0	5.7 ± 0.2	39.3 ± 0.2	0.3 ± 0.0	0.1 ± 0.0	18.6 ± 0.2
HC170-0.5	28.0 ± 0.6	40.2 ± 0.2	53.4 ± 0.9	6.4 ± 0.1	56.1 ± 0.2	0.3 ± 0.0	0.3 ± 0.0	6.0 ± 0.2	30.9 ± 0.2	0.2 ± 0.1	< 0.1 ± 0.2	23.3 ± 0.2
HC200-0.3	39.2 ± 0.8	50.8 ± 2.3	41.7 ± 1.1	7.5 ± 0.4	54.0 ± 0.1	1.2 ± 0.0	0.3 ± 0.0	6.0 ± 0.1	31.0 ± 0.1	0.6 ± 0.0	0.1 ± 0.0	22.6 ± 0.1
HC230-0.1	48.2 ± 1.8	51.7 ± 0.1	41.5 ± 0.2	6.8 ± 0.3	56.1 ± 0.1	2.2 ± 0.1	0.3 ± 0.0	5.9 ± 0.2	28.7 ± 0.2	1.1 ± 0.3	0.1 ± 0.0	23.7 ± 0.2
HC230-0.5	27.2 ± 2.3	59.8 ± 0.3	35.5 ± 0.2	4.7 ± 0.4	62.1 ± 0.2	0.5 ± 0.0	0.3 ± 0.0	6.2 ± 0.2	26.2 ± 0.1	0.6 ± 0.1	< 0.1 ± 0.0	26.2 ± 0.1

^a by difference

determined using a CHNS analyzer (LECO CHNS-932). Proximate analysis was performed according to ASTM methods D3173-11, D3174-11, and D3175-11 to determine the moisture, ash, volatile matter (VM), and fixed carbon (FC) content (by difference). Moreover, thermal analysis was performed in a thermogravimetric analyzer (TG 209, F3, Netzsch, Germany). A sample of 15–20 mg was heated from 30 to 900 °C using a heating rate of 10 °C/min under N₂ flow (1 mL/min). The higher heating value (HHV) of the dried solid samples was determined using Equation (3), which is a correlation for calculating HHV from elemental composition (in percentage) (Channiwala and Parikh, 2002).

$$HHV(MJ/kg) = 0.349C + 1.178H + 0.100S - 0.103O - 0.015N - 0.021Ash \quad (3)$$

The concentrations of other mineral elements were quantified by inductively coupled optical emission spectroscopy (ICP-OES) on a Thermo Fisher Scientific IRIS INTREPID II XDL instrument. Individual chemical species were identified by GC–MS (CP-3800/Saturn 2200 with Varian CP-8200 autosampler injection) (De la Rubia et al., 2018). The NIST 2018 Library was used to assess compounds. Only compounds with a probability of at least 40% were considered. A known volume of liquid sample was digested with 10 mL of concentrated H₂SO₄ in the presence of a copper-based catalyst to determine the ammonium (NH₄-N) and organic nitrogen (organic-N) content (which is converted to ammonium) using the Kjeldahl method. The digested samples were mixed with NaOH (6 N, PanReac) to convert ammonium to ammonia and then distilled into 50 mL of a H₃BO₃ solution, which was titrated with H₂SO₄ (0.02 N, PanReac) to measure the total Kjeldahl nitrogen (TKN). To determine the NH₄⁺-N content, aliquots of process water were used directly in the distillation step without prior digestion. Subsequently, titration was carried out to determine the TKN. Nitrite (NO₂[−]) and nitrate (NO₃[−]) were quantified on a Dionex ICS-900 ion chromatograph with chemical suppression and fitted with a Dionex IonPac AS22 4 × 250 mm column, using a mobile phase (1 mL/min) of 1.4 mM NaHCO₃ and 4.5 mM Na₂CO₃. Ortho-PO₄^{3−} in the process water and leachates was analysed photometrically using a Hach Lange LCK350 cuvette test. The Standards Measurements and Testing (SMT) protocol (Pardo et al., 2004) was applied to the washed hydrochar to analyze P speciation. Total P was extracted by mixing 0.2 g of hydrochar (previously calcined at 450 °C for 3 h) with 20 mL of HCl (3.5 M) under continuous stirring for 16 h at room temperature. Ortho-PO₄^{3−} was extracted by mixing 0.2 g of hydrochar with 20 mL of 1 M HCl under continuous stirring for 16 h at 25 °C.

3. Results and discussion

3.1. Characterization of hydrochars

Table 1 shows the proximate and ultimate analysis of the feedstock and the resulting hydrochars from HTC after 60 min. The raw food waste contained 7.2 wt% solids, with a low FC content owing to the high amount of volatile matter derived from the high content of organic compounds in the feedstock (Liu et al., 2019). The nutrient content was 0.5, 3.1, and 3.8 wt% for P, N, and K, respectively. The main mineral elements were Ca (1.2 wt%), Mg (0.2 wt%), Al (0.1 wt%), and Fe (0.1 wt%). Analysis of the liquid fraction collected from the feedstock showed the presence of different types of long-chain hydrocarbons (in the form of alkyl chain compounds and carboxylic acids), aromatic and non-aromatic nitrogen compounds, as well as different types of aromatic compounds. HHV was in the range of biomass fuels (15–20 MJ/kg) because of its low carbonaceous composition and high oxygen content (Pradhan et al., 2018). Since the feedstock was mainly composed of fruit and vegetable waste, it is expected to contain a significant amount of cellulose, hemicellulose and lignin. The study of the combustion of such food waste by thermogravimetric analysis (TGA) showed a first peak (150–250 °C) related to sugars and cellulose decomposition, followed by a broad second peak (250–300 °C) associated with hemicellulose. The third peak corresponds to lignin, which decomposes over a wide temperature range (300–500 °C) due to its heterogeneity and lack of a defined primary structure (Zhang et al., 2019).

With regard to hydrochar, the mass yield decreased significantly with increasing carbonization temperature, especially in the presence of HCl (Table 1), which promoted degradation reactions and solubilization of organic matter to the process water (Heilmann et al., 2014; Jiang et al., 2010). The FC of hydrochar increased with increasing carbonization temperature because of the volatilization of oxygen-containing functional groups, which may allow for a more constant and stable flame during combustion and a higher fuel firing temperature (He et al., 2013). The ash content in the hydrochar obtained in the absence of acid increased with increasing temperature because the inorganic compounds present in the feedstock remained in the solid phase after thermal treatment. In HCl-mediated HTC, the hydrochar had a lower ash content because of its solubilization in the process water.

The elemental composition of hydrochar showed an increase in the carbon content with increasing carbonization temperature and acid concentration. The hydrogen content was not affected by temperature or acid addition, so the O/C and H/C atomic ratios decreased, indicating an increase in the degree of hydrochar carbonization owing to dehydration,

carboxylation, and condensation reactions (Diaz et al., 2019). The sulphur content remained below 0.3 wt% in all cases. The HHV of hydrochar from acid-free HTC gradually increased with increasing temperature to a value 1.25-fold higher than that of the feedstock. In acid-mediated carbonization, a significant increase in HHV was observed, reaching a value of 26.2 MJ/kg at 230 °C and 0.5 M HCl, related to the low mass yield (27.2 wt%). This HHV value was similar to that of lignite (Engin et al., 2019) and comparable to those reported for the HTC of food waste (20.8–31.1 MJ/kg for a temperature range of 200–300 °C) (Saqib et al., 2019). The FC content of the hydrochar obtained with HCl addition and the reduced values of N, S, and ash contents meet the current parameters of energy recovery from biomass according to ISO 17225–8, making it a promising alternative biofuel.

3.2. Nutrient recovery from hydrochar

The hydrochars obtained by plain HTC were washed with 0.5 M HCl to extract P, N, and K. Fig. 1 shows the distribution of total P (as PO_4^{3-}), N, and K extracted from the leachate, as well as the content of these nutrients retained in the washed hydrochar and the corresponding recovery percentage with respect to the raw feedstock. Most of the P was retained in the hydrochar, increasing in concentration with increasing carbonization temperature. The P content was 64.2% at 170 °C (3.2 g P/kg feedstock) and 99.8% at 230 °C (almost 5 g P/kg feedstock) because of the precipitation of insoluble phosphate salts formed by cations present in the process water such as Ca^{2+} , Mg^{2+} , Al^{3+} , and Fe^{2+} (Dai et al., 2017; Ekpo et al., 2016; Idowu et al., 2017). Acid washing of the hydrochar allowed the recovery of 2.1 g P/kg feedstock at 170 °C and 3.7 g P/kg feedstock at 230 °C in the leachate. Thus, phosphorus recovery by acid washing together with the phosphorus recovered in the process water accounted for approximately 80% of the P contained in the raw food waste working at 170 °C.

Under non-acidic HTC conditions, N and K were mainly extracted in the process water, and their concentrations increased in the hydrochar with increasing temperature, reaching values of 32.7–40.6 wt% and 14.1–24.6 wt%, respectively. In contrast to P, acid washing of hydrochar did not favour the release of N by acid extraction. This behaviour could be related to the initial speciation of N in the feedstock, where proteins are hydrolyzed to amino acids under HTC conditions to be released into the process water. In addition, a higher nitrate content than ammonium causes strong N bonds with dissolved compounds that promote salt precipitation on the hydrochar (Kruse et al., 2016; Peterson et al., 2010; Zhang et al., 2019). The N recovery in the aqueous phases reached values of approximately 77% with respect to the content present in the raw material, irrespective of carbonization. Finally, the recovery of K in the process water, together with the K leached by acid washing of

hydrochar, allowed to recover 93% of this mineral cation.

3.3. Nutrient recovery from process water

3.3.1. Fate of phosphorus

Fig. 2a shows the evolution of the P concentration in the process water, which in all cases was in the form of PO_4^{3-} , throughout the HTC process. In non-acidic HTC reactions, the highest P concentration was reached at 170 °C after 5 min of reaction (0.2 g P/L), equivalent to 2.3 g P/kg feedstock. After 5 min, the P concentration decreased progressively for all the temperatures tested, which can be attributed to the precipitation of P as PO_4^{3-} owing to the presence of mineral elements leached out during the reaction. Fig. 3a and 3b show the fate of cations (Al^{3+} , Ca^{2+} , Fe^{2+} , and Mg^{2+}) in the process water during plain HTC at 170 °C and 230 °C, respectively. At both temperatures, calcium and magnesium ions reached higher concentrations than the iron and aluminium. During the first 30 min of the reaction, a significant decrease in the concentration of Ca^{2+} was observed, related to the observed decrease in the concentration of P. According to Mekmene et al. (2009), calcium-deficient apatite, with a Ca/P molar ratio of 2:1, can precipitate under atmospheric conditions at 37 °C and a pH of approximately 7.5–9. However, hydrothermal conditions have been found to extend these precipitation conditions. Onoda and Yamazaki (2016) were able to precipitate calcium phosphate with a Ca/P molar ratio of up to 3:1 under hydrothermal conditions at 160 °C and at pH values below 6, possibly explaining the fate of dissolved P during HTC of food waste. In our work, at 170 °C, the Ca/P molar ratio decreased to 2.5:1 and the pH of the aqueous phase was 5.4; therefore, it is feasible that the presence of Ca^{2+} favours the concentration of P in the process water. At 230 °C, the pH of the aqueous medium was 5.8, and only a slight decrease in the concentration of both Ca^{2+} and P, equivalent to a Ca/P molar ratio of 2:1, was observed until P was relatively depleted. At this temperature, which favours the retention of P and Ca within the hydrochar, their availability in the process water would be lower.

In HCl-mediated HTC (Fig. 2b), the P concentration in the process water decreased with increasing temperature and, at similar temperatures, increased with increasing HCl concentration. As reported by several authors, the addition of mineral acids during HTC improves the extraction of P from process water in the hydrothermal treatment of organic waste, and this has been tested mainly for various types of manure. Ekpo et al. (2016) observed enhanced P extraction under acidic conditions, as well as temperature dependence, in treating swine manure, obtaining a recovery as high as 94% P using 0.1 M H_2SO_4 at 170 °C. Acid-mediated HTC has also been used for the reclamation of nutrients from cattle manure. Dai et al. (2017) observed a maximum recovery close to 100% P in the process water from HTC mediated by 0.6 M HCl at 190 °C. Qaramaleki et al. (2020) compared the effect of HCl and citric acid on nutrient extraction in process water, obtaining 96% P recovery in process water obtained at 170 °C using 0.5 M HCl; however, in this case, the maximum P recovery (98% of initial P) was achieved under the same conditions using citric acid as the reagent. According to these results and those from our research, the positive effect of HCl addition on P extraction decreases significantly with increasing temperature from 170 to 200 °C and above. In our case, at 170 °C with 0.5 M HCl, the availability of P in the process water increased with increasing reaction time until reaching a concentration of 0.44 g/L (equivalent to 4.9 g P/kg food waste) after 60 min, which was three times higher than that obtained in the experiments without acid addition at the same temperature. However, although P was mainly concentrated in the process water at 230 °C, its trend was different, where we detected both P and the mineral cations at higher concentrations (Fig. 3d) at an almost constant concentration. This trend was opposite that of the plain reactions and could be explained by the non-formation of metal phosphates. As can be seen in Fig. 3c and 3d, the concentration of metal cations (especially Ca^{2+} , Fe^{2+} , and Mg^{2+}) in acidified process water from HTC at 170 °C and 230 °C, respectively, followed the same trend as

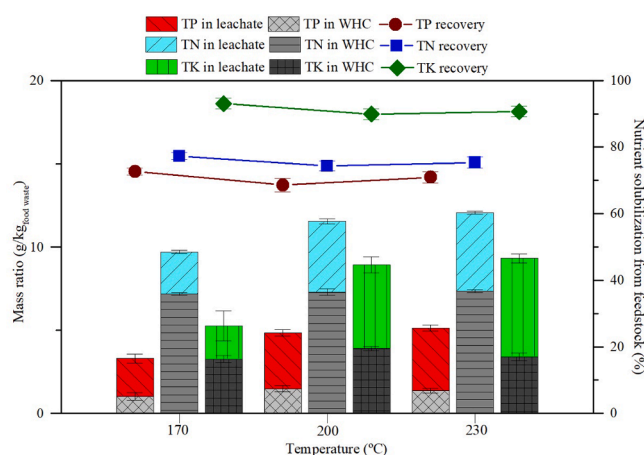


Fig. 1. Total N, P, and K distribution after acid washing of hydrochar and nutrient recovery from raw food waste.

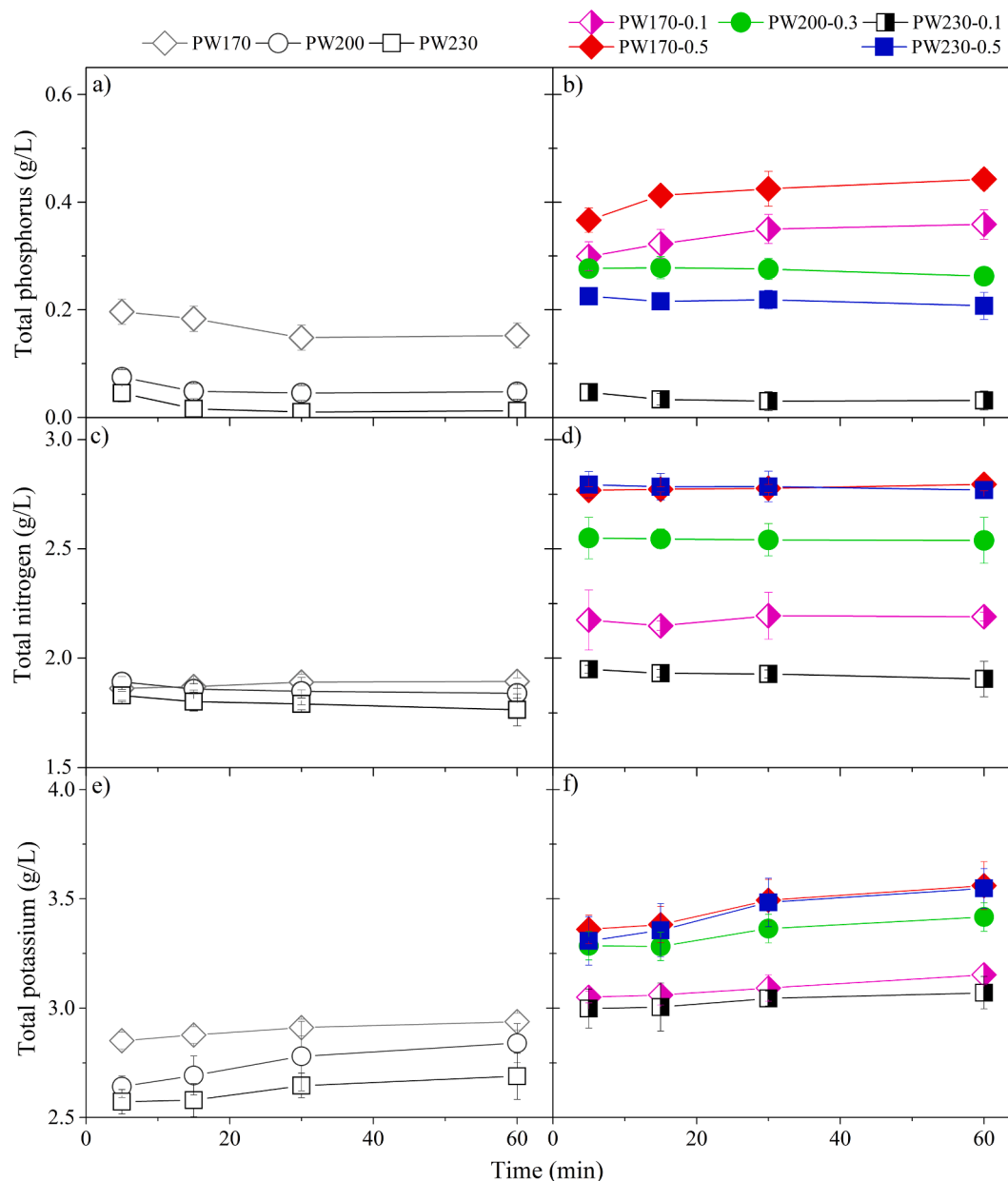


Fig. 2. Time course of phosphorous, nitrogen, and potassium in the process water for HTC reaction (a, c, and e) and HCl-mediated HTC reaction (b, d, and f).

the P concentration, indicating that they were solubilized and that precipitation on the hydrochar did not occur. This is mainly owing to the effect of pH on the phosphate species present in the medium. At pH values below 4.8, phosphate anions were mainly in their monobasic form (H_2PO_4^-), which facilitates the formation of acid phosphates with cations such as Al^{3+} , whose bonding is favoured by the decreased number of OH^- anions (Palacios et al., 2013). However, the formation of phosphates with cations such as Ca^{2+} or Mg^{2+} is not favoured at very acidic pH values because a decrease in the oversaturation of the medium occurs because of protonation of the dibasic phosphate species (HPO_4^{2-}), which is predominant at pH values above 4.8, with which they have more affinity (Mekmene et al., 2009).

Fig. 4a shows the response surface of total P recovery (as $\text{PO}_4\text{-P}$) versus temperature and acid concentration at 60 min, the time at which the highest P concentration was reached in the process water. The evolution of the P recovery was fitted to Equation (4).

$$TP = 2.8283 - 0.01239T - 0.708C + 0.00725TC \quad (4)$$

where T is the HTC temperature ($^{\circ}\text{C}$), C is the HCl concentration (M), and TP is the fraction of total P recovered in the process water. A diagnostic analysis (R^2 99.93% and p -value < 0.05) validated the model and showed that the correlation was well fitted and adequate to predict the evolution of P recovery, which was close to that obtained through the experimental results. P recovery increased with decreasing temperature and increasing HCl addition, reaching 98% recovery of P from food waste at 60 min for 0.5 M HCl-mediated HTC at 170°C . In the non-acid experiments, P recovery was significantly lower (32.9% P recovery in the process water at 170°C). The P recovery obtained using 0.5 M HCl was significantly higher than that obtained by Idowu et al. (2017) using food waste (70% P recovery at 225°C), and even higher than those obtained for other P-rich biowaste such as sewage sludge (82% P recovery after HTC at 230°C) (Munir et al., 2019) or manure (92% P recovery after HTC mediated by 0.1 M H_2SO_4 at 170°C) (Ekpo et al., 2016).

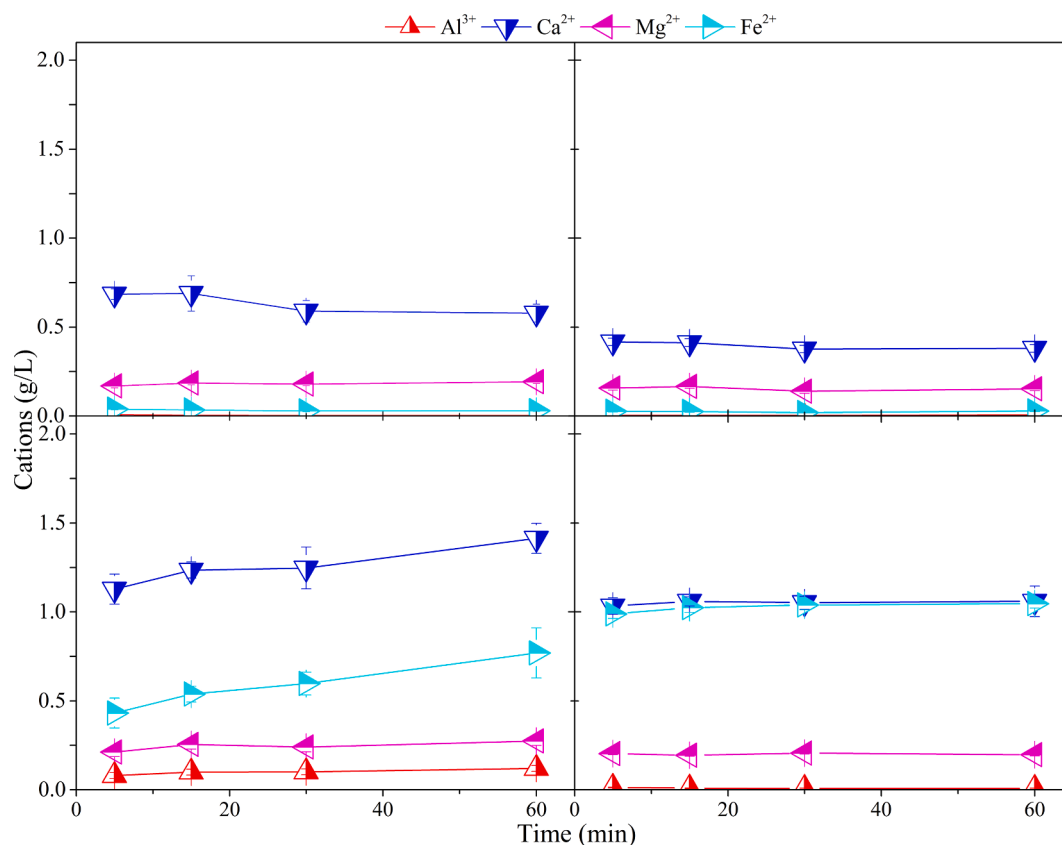


Fig. 3. Time course of the main cations in the process water for HTC carried out at (a) 170 °C and (b) 230 °C and 0.5 M HCl-mediated HTC at (c) 170 °C and (d) 230 °C.

3.3.2. Fate of nitrogen

A complementary analysis of the N recovery in the process water was performed. Fig. 2c and 2d show the evolution of the N concentration in the process water resulting from acid-free and HCl-mediated HTC, respectively. In the acid-free experiments (Fig. 2c), the concentration of dissolved N was similar after 5 min of reaction at the three temperatures studied (1.8 g N/L), with a slight decrease of this concentration in the process water obtained at 200 °C and 230 °C. The fate of N related to HTC has been previously studied by several authors (Ekpo et al., 2015; Idowu et al., 2017; Kruse et al., 2016; Reza et al., 2016), who have related its solubilization to the temperature increase. This difference could be attributed to the effective adsorption properties of the hydrochar, causing the sorption of nitrogen-containing substances at higher temperatures and reaction times (Regmi et al., 2012; Reza et al., 2016).

In the case of HCl-mediated HTC (Fig. 2d), the acid had a remarkable effect on the increased N concentration in the process water, mainly owing to the hydrolysis of nitrogen-bearing organic compounds (Dai et al., 2017; Ekpo et al., 2016). With the lowest HCl addition (0.1 M), a 1.19-fold increase in the maximum N concentration was found in the process water obtained at 170 °C compared to the plain reactions, showing again that an increase in HTC temperature was not associated with increased N leaching. However, when the HCl concentration was increased to 0.5 M, the same concentration of dissolved N was obtained at 170 and 230 °C. Under these conditions, the N concentration in the process water reached 2.8 g/L (corresponding to 30.4 g N/kg food waste), showing no significant differences over time and showing that the effect of acid allows the release of N during HTC. A similar effect of acid-mediated HTC on nutrient recovery from manure has been observed by some authors. Ekpo et al. (2016) reported that a milder HTC temperature is more favourable for maximizing N extraction from swine manure in the presence of 0.1 M H₂SO₄. Dai et al. (2017) concluded that an increase in HCl concentration for HTC at constant temperature was

essential for increasing the release of N (64% N in feedstock), and Qaramaleki et al. (2020) observed that, in contrast to P recovery, the best N extraction results in the process water were obtained at 200 °C using 0.5 M HCl instead of citric acid (approximately 60% N content of the raw material).

The analysis of the N compounds present in the process water (Fig. 5) showed that the principal nitrogen species obtained in plain HTC were nitrates (74–78%) and ammonium (21–23%), regardless of temperature. In the HCl-mediated HTC, the N concentration in form of nitrogen-bearing organic compounds increased up to 55% at 170 °C and 0.5 M HCl, which could be owing to sequential decomposition of proteins to NH₄-N under acidic hydrothermal conditions (Dai et al., 2017; Kruse et al., 2016; Sato et al., 2004). During reactions with 0.5 M HCl, the presence of nitrates decreased significantly (24–27%).

Fig. 4b and 4c show the response surface of N recovery in the process water (as total nitrogen and ammonia nitrogen, respectively) after 60 min of reaction. Equations (5) and (6) describe the evolution of total N and NH₄-N recovery in the aqueous phase as a function of temperature and HCl concentration, respectively. The statistical parameters obtained (R² 99.7% and p < 0.05) validate the response surfaces shown.

$$TN = 1.26 - 0.0026T - 0.46C + 0.0057C^2 \quad (5)$$

$$TNH_4 - N = 0.18 - 0.00015T - 0.23C + 0.0015C^2 \quad (6)$$

where TN_L and TNH_4-N are the fractions of total N and NH₄⁺, respectively, as N concentration recovered in the process water.

It is apparent that the HCl concentration is crucial for the release of N into the process water. The maximum N recovery in this phase was achieved with 0.5 M HCl-mediated HTC at 170 °C, which was slightly higher than that obtained with 0.5 M HCl at 230 °C. In this sense, HCl-mediated HTC of food waste seems to be a promising process that allows for better N recovery compared to plain HTC of food waste (50% N

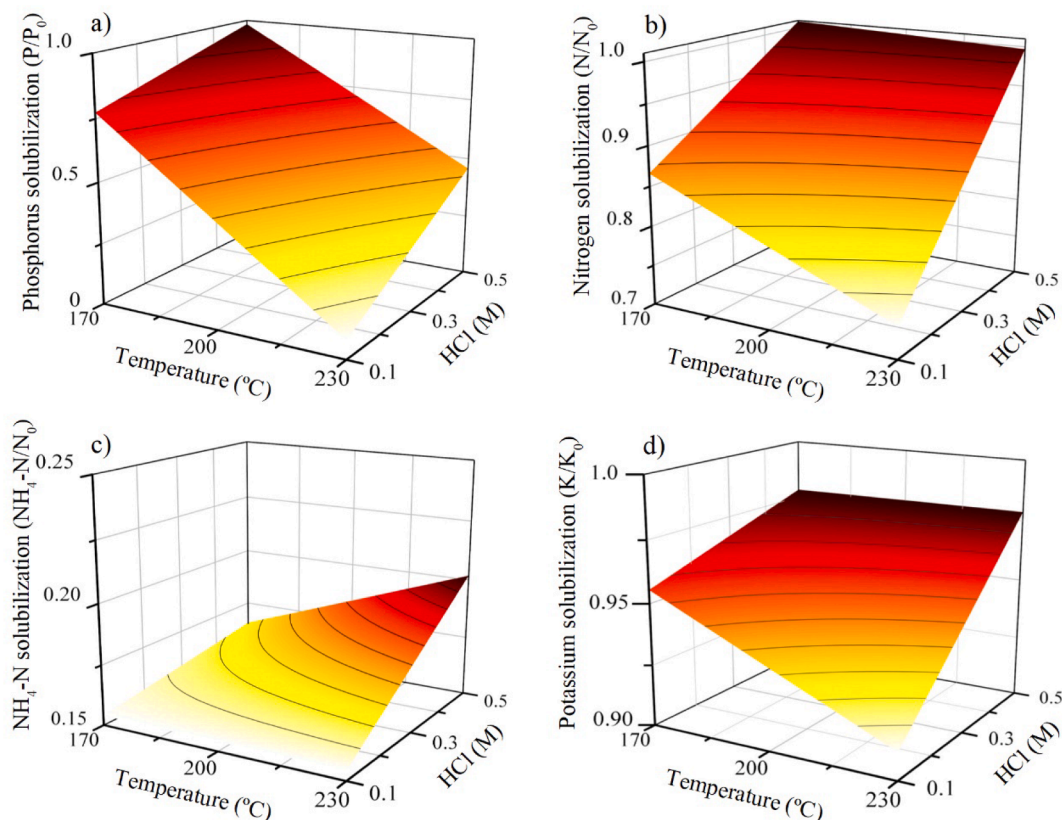


Fig. 4. Response surface of (a) phosphorus (in form of *ortho*-phosphate), (b) nitrogen, (c) $\text{NH}_4\text{-N}$, and (d) potassium recovery in process water after 60 min of HCl-mediated HTC.

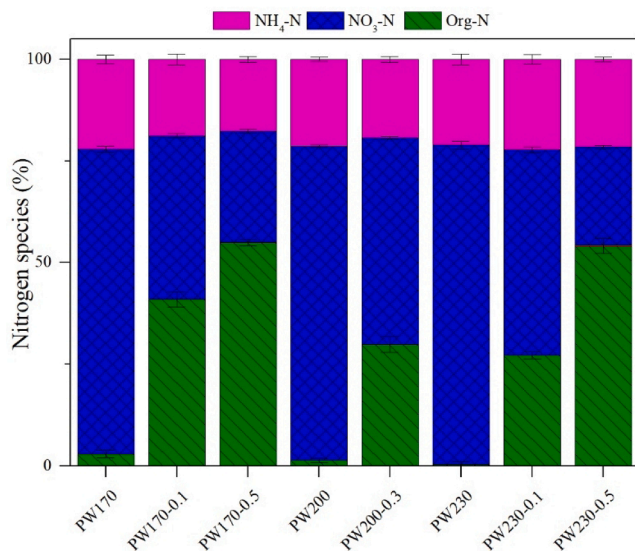


Fig. 5. Distribution of nitrogen species in process water after HTC reaction.

recovery in process water) (Idowu et al., 2017). However, only 16% of the TN was recovered as $\text{NH}_4\text{-N}$ because the corresponding transformation of the released organic-N to $\text{NH}_4\text{-N}$ is favoured with increasing reaction time and HTC temperature. For this reason, at 230 °C and 0.5 M HCl, the amount of $\text{NH}_4\text{-N}$ in the process water increased by 7% over the same reaction time, which was 22% higher than that obtained at 170 °C.

3.3.3. Fate of potassium

The highest K extraction in the process water was observed at the lowest temperature (170 °C), and its concentration increased with reaction time in all cases (Fig. 2e and 2f). These results were expected because of the high solubility of K in water. Acid-mediated HTC enhanced the solubility of K, obtaining the highest K concentration at 170 °C using 0.5 M HCl (37.5 g K/kg food waste). The response surface study for K recovery (Fig. 4d) yielded Equation (7) (R^2 99.7% and $p < 0.05$).

$$TK = 1.11 - 0.00093T - 0.26C + 0.0019TC \quad (7)$$

where TK is the fraction of total K recovered in the process water. As can be seen, K was almost completely extracted (more than 90% of the initial K) for all of the temperatures and acid concentration used, with the concentration being the most relevant variable. The highest K recovery in the process water (98% of the K in the feedstock) was achieved with 0.5 M HCl-mediated HTC, irrespective of the temperature used.

4. Conclusions

Hydrothermal carbonization has emerged as an alternative to valorize food waste into solid biofuels; it also allows for nutrient recovery. The solubilization of nutrients by plain HTC was temperature-dependent. In general, mild temperatures (170 °C) are recommended to improve nutrient solubilization after an optimal reaction time of 60 min. However, the addition of HCl during HTC was crucial for maximising N (as organic-N and NH_4^+), P (as PO_4^{3-}), and K recovery directly in the process water. Additionally, HTC allows the production of hydrochar, which has attractive characteristics as a biofuel for industry. Considering these results, HCl-mediated HTC facilitates nutrient recovery from food waste and upgrades the resulting hydrochar.

CRediT authorship contribution statement

Andres Sarrion: Investigation, Formal analysis, Writing – original draft. : **Elena Diaz:** Conceptualization, Formal analysis, Funding acquisition, Methodology, Resources, Writing – review & editing, Supervision. **M. Angeles Rubia:** Funding acquisition, Writing – review & editing, Supervision. **Angel F. Mohedano:** Conceptualization, Funding acquisition, Methodology, Resources, Writing – review & editing, Supervision, Project administration.

Declaration of Competing Interest

The authors declare that they have no known competing financial interests or personal relationships that could have appeared to influence the work reported in this paper.

Acknowledgements

The authors greatly appreciate funding from Spanish MICINN (Project PID2019-108445RB-I00) and Madrid Regional Government (Project S2018/EMT-4344). A. Sarrion wishes to thank the Spanish MICINN and ESF for a research grant (BES-2017-081515). The authors thank Silvia Rodríguez for her valuable help.

Appendix A. Supplementary data

Supplementary data to this article can be found online at <https://doi.org/10.1016/j.biortech.2021.125954>.

References

- Becker, G.C., Wüst, D., Köhler, H., Lautenbach, A., Kruse, A., 2019. Novel approach of phosphate-reclamation as struvite from sewage sludge by utilising hydrothermal carbonization. *J. Environ. Manage.* 238, 119–125. <https://doi.org/10.1016/j.jenvman.2019.02.121>.
- Berge, N.D., Ro, K.S., Mao, J., Flora, J.R.V., Chappell, M.A., Bae, S., 2011. Hydrothermal Carbonization of Municipal Waste Streams. *Environ. Sci. Technol.* 45 (13), 5696–5703. <https://doi.org/10.1021/es2004528>.
- Celletti, S., Lanz, M., Bergamo, A., Benedetti, V., Basso, D., Baratieri, M., Cesco, S., Mimmo, T., 2021. Evaluating the Aqueous Phase From Hydrothermal Carbonization of Cow Manure Digestate as Possible Fertilizer Solution for Plant Growth. *Front. Plant Sci.* 1317. <https://doi.org/10.3389/fpls.2021.687434>.
- Channiwala, S.A., Parikh, P.P., 2002. A unified correlation for estimating HHV of solid, liquid and gaseous fuels. *Fuel* 81 (8), 1051–1063. [https://doi.org/10.1016/S0016-2361\(01\)00131-4](https://doi.org/10.1016/S0016-2361(01)00131-4).
- Cieslik, B., Konieczka, P., 2017. A review of phosphorus recovery methods at various steps of wastewater treatment and sewage sludge management. The concept of “no solid waste generation” and analytical methods. *J. Clean. Prod.* 142, 1728–1740. <https://doi.org/10.1016/j.jclepro.2016.11.116>.
- Dai, L., Yang, B., Li, H., Tan, F., Zhu, N., Zhu, Q., He, M., Ran, Y., Hu, G., 2017. A synergistic combination of nutrient reclamation from manure and resultant hydrochar upgradation by acid-supported hydrothermal carbonization. *Bioresour. Technol.* 243, 860–866. <https://doi.org/10.1016/j.biortech.2017.07.016>.
- De la Rubia, M.A., Villamil, J.A., Rodriguez, J.J., Borja, R., Mohedano, A.F., 2018. Mesophilic anaerobic co-digestion of the organic fraction of municipal solid waste with the liquid fraction from hydrothermal carbonization of sewage sludge. *Waste Manag.* 76, 315–322. <https://doi.org/10.1016/j.wasman.2018.02.046>.
- Diaz, E., Manzano, F.J., Villamil, J., Rodriguez, J.J., F. Mohedano, A., 2019. Low-cost activated grape seed-derived hydrochar through hydrothermal carbonization and chemical activation for sulfamethoxazole adsorption. *Appl. Sci.* 9, 5127. <https://doi.org/10.3390/app9235127>.
- Ekpo, U., Ross, A.B., Camargo-Valero, M.A., Fletcher, L.A., 2016. Influence of pH on hydrothermal treatment of swine manure: Impact on extraction of nitrogen and phosphorus in process water. *Bioresour. Technol.* 214, 637–644. <https://doi.org/10.1016/j.biortech.2016.05.012>.
- Ekpo, U., Ross, A.B., Camargo-Valero, M.A., Williams, P.T., 2015. A comparison of product yields and inorganic content in process streams following thermal hydrolysis and hydrothermal processing of microalgae, manure and digestate. *Bioresour. Technol.* 200, 951–960. <https://doi.org/10.1016/j.biortech.2015.11.018>.
- Engin, B., Atakül, H., Ünü, A., Olgun, Z., 2019. CFB combustion of low-grade lignites: Operating stability and emissions. *J. Energy Inst.* 92 (3), 542–553. <https://doi.org/10.1016/j.joei.2018.04.004>.
- European Commission, 2020. A new circular economy action plan for a cleaner and more competitive Europe. Brussels. <https://doi.org/https://www.un.org/sustainabledevelopment/sustainable-consumption-production/>.
- European Commission, 2018. DIRECTIVE (EU) 2018/851 of the European Parliament and the Council of 30 May 2018 amending Directive 2008/98/EC on waste. *Off. J. Eur. Union*, 150/109.
- Fernandez, M.E., Ledesma, B., Román, S., Bonelli, P.R., Cukierman, A.L., 2015. Development and characterization of activated hydrochars from orange peels as potential adsorbents for emerging organic contaminants. *Bioresour. Technol.* 183, 221–228. <https://doi.org/10.1016/j.biortech.2015.02.035>.
- Funke, A., Ziegler, F., 2011. Heat of reaction measurements for hydrothermal carbonization of biomass. *Bioresour. Technol.* 102 (16), 7595–7598. <https://doi.org/10.1016/j.biortech.2011.05.016>.
- Ge, X., Ge, M., Chen, X., Qian, C., Liu, X., Zhou, S., 2020. Facile synthesis of hydrochar supported copper nanocatalyst for Ullmann CN coupling reaction in water. *Mol. Catal.* 484, 110726. <https://doi.org/10.1016/j.mcat.2019.110726>.
- He, C., Giannis, A., Wang, J.Y., 2013. Conversion of sewage sludge to clean solid fuel using hydrothermal carbonization: Hydrochar fuel characteristics and combustion behavior. *Appl. Energy* 111, 257–266. <https://doi.org/10.1016/j.apenergy.2013.04.084>.
- Heilmann, S.M., Molde, J.S., Timler, J.G., Wood, B.M., Mikula, A.L., Vozhdayev, G.V., Colosky, E.C., Spokas, K.A., Valentas, K.J., 2014. Phosphorus reclamation through hydrothermal carbonization of animal manures. *Environ. Sci. Technol.* 48 (17), 10323–10329. <https://doi.org/10.1021/es501872k>.
- Iidowu, I., Li, L., Flora, J.R.V., Pellechia, P.J., Darko, S.A., Ro, K.S., Berge, N.D., 2017. Hydrothermal carbonization of food waste for nutrient recovery and reuse. *Waste Manag.* 105, 566–574. <https://doi.org/10.1016/j.wasman.2017.08.051>.
- Jiang, Z., Meng, D., Mu, H., Yoshikawa, K., 2010. Study on the hydrothermal drying technology of sewage sludge. *Sci. China Technol. Sci.* 53 (1), 160–163. <https://doi.org/10.1007/s11431-009-0423-7>.
- Kjerstadhus, H., Haghighatafshar, S., Davidsson, Å., 2015. Potential for nutrient recovery and biogas production from blackwater, food waste and greywater in urban source control systems. *Environ. Technol.* 36 (13), 1707–1720. <https://doi.org/10.1080/09593330.2015.1007089>.
- Kruse, A., Koch, F., Stelzl, K., Wüst, D., Zeller, M., 2016. Fate of nitrogen during hydrothermal carbonization. *Energy and Fuels* 30 (10), 8037–8042. <https://doi.org/10.1021/acs.energyfuels.6b01312>.
- Kumar, M., Olajire Oyedun, A., Kumar, A., 2018. A review on the current status of various hydrothermal technologies on biomass feedstock. *Renew. Sustain. Energy Rev.* 81, 1742–1770. <https://doi.org/10.1016/j.rser.2017.05.270>.
- Liu, Z., Zhang, Y., Liu, Z., 2019. Comparative production of biochars from corn stalk and cow manure. *Bioresour. Technol.* 291, 121855. <https://doi.org/10.1016/j.biortech.2019.121855>.
- Mekmene, O., Quillard, S., Rouillon, T., Boulter, J.M., Piot, M., Gaucheron, F., 2009. Effects of pH and Ca/P molar ratio on the quantity and crystalline structure of calcium phosphates obtained from aqueous solutions. *Dairy Sci. Technol.* 89 (3–4), 301–316. <https://doi.org/10.1051/dst/2009019>.
- Munir, M.T., Li, B., Mardon, I., Young, B.R., Baroutian, S., 2019. Integrating wet oxidation and struvite precipitation for sewage sludge treatment and phosphorus recovery. *J. Clean. Prod.* 232, 1043–1052. <https://doi.org/10.1016/j.jclepro.2019.06.007>.
- Niu, Z., Feng, W., Huang, H., Wang, B., Chen, L., Miao, Y., Su, S., 2020. Green synthesis of a novel Mn–Zn ferrite/biochar composite from waste batteries and pine sawdust for Pb²⁺ removal. *Chemosphere* 252, 126529. <https://doi.org/10.1016/j.chemosphere.2020.126529>.
- Onoda, H., Yamazaki, S., 2016. Homogenous hydrothermal synthesis of calcium phosphate with calcium carbonate and corbicula shells. *J. Asian Ceram. Soc.* 4 (4), 403–406. <https://doi.org/10.1016/j.jascer.2016.10.001>.
- Ostadi, A., Javanmard, A., Amani Machiani, M., Morshedloo, M.R., Nouraein, M., Rasouli, F., Maggi, F., 2020. Effect of different fertilizer sources and harvesting time on the growth characteristics, nutrient uptakes, essential oil productivity and composition of *Mentha x piperita* L. *Ind. Crops Prod.* 148, 112290. <https://doi.org/10.1016/j.indcrop.2020.112290>.
- Palacios, E., Leret, P., De La Mata, M.J., Fernández, J.F., De Aza, A.H., Rodríguez, M.A., 2013. Influence of the pH and ageing time on the acid aluminum phosphate synthesized by precipitation. *CrystEngComm* 15, 3359–3365. <https://doi.org/10.1039/c3ce00011g>.
- Panigrahi, S., Dubey, B.K., 2019. A critical review on operating parameters and strategies to improve the biogas yield from anaerobic digestion of organic fraction of municipal solid waste. *Renew. Energy* 143, 779–797. <https://doi.org/10.1016/j.renene.2019.05.040>.
- Pardo, P., Rauret, G., López-Sánchez, J.F., 2004. Shortened screening method for phosphorus fractionation in sediments: A complementary approach to the standards, measurements and testing harmonised protocol. *Anal. Chim. Acta* 508 (2), 201–206. <https://doi.org/10.1016/j.aca.2003.11.005>.
- Peterson, A.A., Lachance, R.P., Tester, J.W., 2010. Kinetic evidence of the maillard reaction in hydrothermal biomass processing: Glucose-glycine interactions in high-temperature, high-pressure water. *Ind. Eng. Chem. Res.* 49 (5), 2107–2117. <https://doi.org/10.1021/ie9014809>.
- Pradhan, P., Mahajani, S.M., Arora, A., 2018. Production and utilization of fuel pellets from biomass: A review. *Fuel Process. Technol.* 181, 215–232. <https://doi.org/10.1016/j.fuproc.2018.09.021>.
- Qaramaleki, S.V., Villamil, J.A., Mohedano, A.F., Coronella, C.J., 2020. Factors affecting solubilization of phosphorus and nitrogen through hydrothermal carbonization of animal manure. *ACS Sustain. Chem. Eng.* 8, 12462–12470. <https://doi.org/10.1021/acscuschemeng.0c03268>.
- Regmi, P., Garcia Moscoso, J.L., Kumar, S., Cao, X., Mao, J., Schafran, G., 2012. Removal of copper and cadmium from aqueous solution using switchgrass biochar produced

- via hydrothermal carbonization process. *J. Environ. Manage.* 109, 61–69. <https://doi.org/10.1016/j.jenvman.2012.04.047>.
- Reza, M.T., Freitas, A., Yang, X., Hiiibel, S., Lin, H., Coronella, C.J., 2016. Hydrothermal carbonization (HTC) of cow manure: Carbon and nitrogen distributions in HTC products. *Environ. Prog. Sustain. Energy* 35, 1002–1011. <https://doi.org/10.1002/ep.12312>.
- Saqib, N.U., Sharma, H.B., Baroutian, S., Dubey, B., Sarmah, A.K., 2019. Valorisation of food waste via hydrothermal carbonisation and techno-economic feasibility assessment. *Sci. Total Environ.* 690, 261–276. <https://doi.org/10.1016/j.scitotenv.2019.06.484>.
- Sato, N., Quitain, A.T., Kang, K., Daimon, H., Fujie, K., 2004. Reaction kinetics of amino acid decomposition in high-temperature and high-pressure water. *Ind. Eng. Chem. Res.* 43 (13), 3217–3222. <https://doi.org/10.1021/ie020733n>.
- Sharma, H.B., Panigrahi, S., Dubey, B.K., 2019. Hydrothermal carbonization of yard waste for solid bio-fuel production: Study on combustion kinetic, energy properties, grindability and flowability of hydrochar. *Waste Manag.* 91, 108–119. <https://doi.org/10.1016/j.wasman.2019.04.056>.
- Shiba, N.C., Ntuli, F., 2017. Extraction and precipitation of phosphorus from sewage sludge. *Waste Manag.* 60, 191–200. <https://doi.org/10.1016/j.wasman.2016.07.031>.
- Szögi, A.A., Vanotti, M.B., Hunt, P.G., 2015. Phosphorus recovery from pig manure solids prior to land application. *J. Environ. Manage.* 157, 1–7. <https://doi.org/10.1016/j.jenvman.2015.04.010>.
- Tang, Z., Li, W., Tam, V.W.Y., Xue, C., 2020. Advanced progress in recycling municipal and construction solid wastes for manufacturing sustainable construction materials. *Resour. Conserv. Recycl. X* 6, 100036. <https://doi.org/10.1016/j.rcrx.2020.100036>.
- Vallero, D.A., 2019. In: *Waste*. Elsevier, pp. 171–198.
- Wilk, M., Magdziarz, A., Jayaraman, K., Szymańska-Chargot, M., Gókalp, I., 2019. Hydrothermal carbonization characteristics of sewage sludge and lignocellulosic biomass. A comparative study. *Biomass and Bioenergy* 120, 166–175. <https://doi.org/10.1016/j.biombioe.2018.11.016>.
- World bank, 2018. What a Waste: an updated look into the future of solid waste management [WWW Document]. accessed 3.20.20. <https://www.worldbank.org/en/news/immersive-story/2018/09/20/what-a-waste-an-updated-look-into-the-future-of-solid-waste-management>.
- Xia, Y., Luo, H., Li, D., Chen, Z., Yang, S., Liu, Z., Yang, T., Gai, C., 2020. Efficient immobilization of toxic heavy metals in multi-contaminated agricultural soils by amino-functionalized hydrochar: Performance, plant responses and immobilization mechanisms. *Environ. Pollut.* 261, 114217. <https://doi.org/10.1016/j.envpol.2020.114217>.
- Yu, Y., Lei, Z., Yuan, T., Jiang, Y., Chen, N., Feng, C., Shimizu, K., Zhang, Z., 2017. Simultaneous phosphorus and nitrogen recovery from anaerobically digested sludge using a hybrid system coupling hydrothermal pretreatment with MAP precipitation. *Bioresour. Technol.* 243, 634–640. <https://doi.org/10.1016/j.biortech.2017.06.178>.
- Zhang, Y., Jiang, Q., Xie, W., Wang, Y., Kang, J., 2019. Effects of temperature, time and acidity of hydrothermal carbonization on the hydrochar properties and nitrogen recovery from corn stover. *Biomass and Bioenergy* 122, 175–182. <https://doi.org/10.1016/j.biombioe.2019.01.035>.
- Zhao, X., Becker, G.C., Faweya, N., Rodriguez Correa, C., Yang, S., Xie, X., Kruse, A., 2018. Fertilizer and activated carbon production by hydrothermal carbonization of digestate. *Biomass Convers. Biorefinery* 8, 423–436. <https://doi.org/10.1007/s13399-017-0291-5>.